water

MDPI

Article

Determining Groundwater Drought Relative to the Opening of a River Barrage in Korea

Sul-Min Yun [1], Ji-Hye Jeong [2], Hang-Tak Jeon [3], Jae-Yeol Cheong [4,*] and Se-Yeong Hamm [5,*]

[1] Department of Geological Sciences, BK21 School of Earth and Environmental Systems, Pusan National University, Busan 46241, Republic of Korea; ehdls91@naver.com
[2] Korea Water Resources Corporation, Daejeon 34350, Republic of Korea; jhjeong@kwater.or.kr
[3] Geo Science, Co., Busan 46241, Republic of Korea; jeonhangtak@gmail.com
[4] Radwaste Technology & Research Institute, Korea Radioactive Waste Agency, Gyeongju 38062, Republic of Korea
[5] Department of Geological Sciences, Pusan National University, Busan 46241, Republic of Korea
* Correspondence: jjy@korad.or.kr (J.-Y.C.); hsy@pusan.ac.kr (S.-Y.H.)

Abstract: Groundwater droughts are one of the natural disasters that raise serious water issues for humans, and are increasing in frequency due to global climate change. In order to identify groundwater droughts, we recorded groundwater level fluctuations upstream at Changnyeong-Haman River barrage from May 2012 to October 2020, based on the groundwater level characteristics and Nakdong River stages. Next, we grouped groundwater levels by K-means clustering, converted groundwater levels to kernel density estimation (KDE), and calculated a standardized groundwater level index (SGLI). Finally, we judged groundwater drought by using the SGLI values corresponding to the opening and closing of the barrage. In the study area, the SGLI criteria for discriminating groundwater drought were −0.674 (caution), −1.282 (severe), and −1.645 (very severe), respectively, corresponding to the 25th, 10th, and 5th percentiles. Based on the SGLI values, groundwater levels on the monitoring wells mostly lie below the 25th percentile during the five opening periods of the barrage. According to cross-correlation analysis, the groundwater level sensitively reacted with the river stage, which influenced groundwater drought. As a result, the SGLI along with the river stages was verified as an efficient tool for evaluating groundwater drought as well as for appropriately operating the barrage.

Keywords: groundwater drought; standardized groundwater level index (SGLI); kernel density estimation (KDE); K-means cluster analysis; cross correlation analysis; river barrage

check for updates

Citation: Yun, S.-M.; Jeong, J.-H.; Jeon, H.-T.; Cheong, J.-Y.; Hamm, S.-Y. Determining Groundwater Drought Relative to the Opening of a River Barrage in Korea. *Water* **2023**, *15*, 2658. https://doi.org/10.3390/w15142658

Academic Editor: Adriana Bruggeman

Received: 28 June 2023
Revised: 20 July 2023
Accepted: 21 July 2023
Published: 22 July 2023

Copyright: © 2023 by the authors. Licensee MDPI, Basel, Switzerland. This article is an open access article distributed under the terms and conditions of the Creative Commons Attribution (CC BY) license (https://creativecommons.org/licenses/by/4.0/).

1. Introduction

Droughts are a tremendous natural disaster that have threatened mankind throughout historical eras and are anticipated to increase in frequency and strength owing to global climate change [1]. Drought is defined as a lack of available water resources (river water, surface storage water, and groundwater) owing to severely decreased precipitation rates. Korea experienced droughts in 1968, 1978, 1982, 1994–1995, 2000–2001, and 2008, with a shortened drought cycle of 5–6 years after the 1900s. During a drought, the river flow rate is determined at flood control stations, and surface dams are helpful in overcoming the deficit in water resources, depending on the amount of reservoir water relative to water demand. Using the standardized precipitation index (SPI), a drought can be evaluated at its beginning and end by its intensity and magnitude [2].

Groundwater reserved in aquifers also decreases because of decreased precipitation due to the decline in groundwater level and outflow from aquifers [3,4]. This is called a groundwater drought and affects the groundwater system for several months to years [5]. In addition, when a drought occurs, the demand for groundwater greatly increases owing

to a shortage of surface water. Groundwater droughts are increasing in frequency owing to global climate change and raises serious concerns about water issues for humans.

Several scientists have proposed some indices for evaluating groundwater drought (e.g., [6–9]). Bloomfield and Marchant [6] proposed the standardised groundwater level index (SGLI) for discriminating groundwater drought using groundwater level data from 14 locations in the UK over 103 years, as well as the SPI for evaluating drought. The USGS provides the current percentile of the groundwater level for each station through an integrated analysis of groundwater monitoring data, and the state governments of the United States determine groundwater drought based on the evaluation data provided by the USGS (http://pr.water.usgs.gov/drought/drought.html (accessed on 16 January 2021)). Rahim et al. [7] evaluated groundwater drought in Pakistan using the standardised water level index and SPI. Using a simple distributed water balance model, Medicino et al. [8] concluded that the groundwater resource index is more appropriate than the SPI for predicting summer drought in the Mediterranean region. Kumar et al. [9] confirmed that the SPI cannot be applied to the prediction of groundwater drought by verifying it based on 2000 groundwater data from Germany and the Netherlands. In contrast, Bidwell [10] developed an autoregressive, moving-average, exogenous-variable (ARMAX) prediction equation using the eigenvalues of aquifer dynamics, and predicted monthly groundwater levels using an equation for groundwater management during the drought period in Canterbury, New Zealand. For drought prediction and warning purposes, Goodarzi et al. [11] analysed groundwater drought based on the groundwater recharge drought index from 30-years groundwater recharge data and separated drought caused by artificial activity from natural drought. In addition, Osman et al. [12] predicted accurate groundwater levels in Selangor, Malaysia by using extreme gradient boosting (Xgboost) model and Osman et al. [13] summarised the most common artificial intelligence methodologies for forecasting groundwater level.

In Korea, Song et al. [14] evaluated the effect of drought on the groundwater system of Jeju Island based on the relationship between the monthly drought index and groundwater-level fluctuations due to monthly mean precipitation. Yang et al. [15] developed a drought vulnerability index using a trend test and estimated the drought vulnerability index for Nakdong and Geum river watersheds in Korea by considering groundwater levels. Kim et al. [16] evaluated drought using the relationship between the SPI and groundwater level data, and proposed drought index wells.

Numerous researchers have studied the relationship between groundwater and surface water [17–25]. Oh et al. [21] examined the effects of the construction of Changnyeong–Haman River barrage in Korea on the interaction between rivers and aquifers. Oh et al. [22] also evaluated groundwater level, river stage, and precipitation data near Changnyeong–Haman River barrage for three years, from 1 July 2012 to 30 June 2015, using dynamic factor and wavelet analyses.

This study aims to characterize the groundwater levels near Nakdong River by classifying the groundwater levels using K-means clustering as well as using the groundwater level characteristics and the river stage. For identifying groundwater drought, the groundwater levels are converted to KDE and the SGLI values are estimated by considering the opening and closing of the barrage on Nakdong River.

2. Methods

2.1. Cross-Correlation Analysis

Cross-correlation analysis was conducted to interpret the link between the input variable x (e.g., river stage) and the output variable y (e.g., groundwater level), utilising the lag time (h) and cross-correlation function [26–28]. The cross-correlation coefficient r_{xy} is expressed as follows:

$$r_{xy} = \frac{cov(x_i, y_{i+k})}{\sigma_{x_i}\sigma_{y_{i+k}}} \quad (1)$$

$$cov(x_i, y_{i+k}) = \sum_{i=i}^{n-k} x_i y_{i+k} - \frac{1}{n-k}\left(\sum_{i=1}^{n-k} y_i\right)\left(\sum_{i=k+1}^{n} y_i\right) \quad (2)$$

$$\sigma_{x_i} = \sqrt{\sum_{i=1}^{n-k} {x_i}^2 - \frac{1}{n-k}\left(\sum_{i=1}^{n-k} x_i\right)^2} \quad (3)$$

$$\sigma_{y_{i+k}} = \sqrt{\sum_{i=k+1}^{n} {y_i}^2 - \frac{1}{n-k}\left(\sum_{i=k+1}^{n} y_i\right)^2} \quad (4)$$

where k is the lag number interval between points x_i and x_{i+k} in the time series, n is the total number of time series, and $cov(x_i, y_{i+k})$ is the covariance between the overlapping portions of sequences x and y. σ_{x_i} and $\sigma_{y_{i+k}}$ are x_i and y_{i+k} in the time series, respectively. The lag time (or delay time), calculated using Equation (1) uses the time lag between k = 0 and the time of the maximum cross-correlation, indicating a faster response and stress transfer in a system with a shorter lag time [28].

2.2. K-Means Cluster Analysis

Because of the different distances from the river, the groundwater levels at the wells responded differently to changes in the river water level. For the K-means clustering analysis, the similarity measurement of cluster analysis is first performed to normalise groundwater levels at different locations using a dynamic time warping algorithm that finds a matrix path or matches a path [29]. To measure the similarity between the time-series pairs ($S = \{S_1, \ldots, S_i, \ldots, S_{Ns}\}$ and $R = \{R_1, \ldots, R_j, \ldots, R_{Ns}\}$), dynamic time warping finds an appropriate matrix that is applied to both local distortions (stretched and compressed parts) and phase correction of the total parts by minimising the W^* cumulative squared distance:

$$W^*(S,\ R) = \underset{W \in P}{argmin} \sum_{(i,j)\in W} d(S_i,\ R_j)^2 \quad (5)$$

In the next step, the normalised time-series data were clustered using the k-means clustering algorithm, which minimises the variance in the cluster. The Euclidean distance was used in the normalisation step when the time series was readjusted.

$$V = \sum_{i=1}^{k} \sum_{\hat{S}^n \in C^i} \|\hat{S}^n - \mu^i\|^2 \quad (6)$$

Here, C^i is the i-th cluster of the mean μ^i.

2.3. Standardized Groundwater Level Index (SGLI)

The SGLI determines groundwater drought by comparing high and low groundwater levels relative to the normal groundwater level [6] and is calculated similarly to the SPI method [2]. SGLI adds a process to normalise the percentile by applying an inverse normal cumulative distribution function. This method has the advantage of determining the groundwater level compared to an average year, reflecting seasonal periodicity. In addition, it normalises the groundwater level of monitoring wells with different water elevations and fluctuations to determine groundwater drought.

In this study, the groundwater level histogram was converted to a probability density function (PDF) using kernel density estimation (KDE), a type of nonparametric estimation. KDE can reproduce the histogram of the original data by improving the limitations of the histogram. For random variable X, the PDF using KDE is defined as follows [30]:

$$\hat{f}_h(X) = \frac{1}{n}\sum_{i=1}^{n} K_h(X - x_i) = \frac{1}{nh}\sum_{i=1}^{n} K\left(\frac{X - x_i}{h}\right) \quad (7)$$

Here, for the observed groundwater level data x_1, x_2, …, x_n, h is the bandwidth of the kernel density function (KDF) and is a parameter that adjusts the smoothness of the kernel. For the PDF $f(x)$, the probability P $(a \leq x \leq b)$ that the probability variable x will be included in the interval $[a, b]$, is:

$$P\ (a \leq X \leq b) = \int_a^b f(x)dx \tag{8}$$

In this circumstance,

$$f(x) \geq 0 \qquad \text{for real number x} \tag{9}$$

$$\int_{-\infty}^{\infty} f(x)dx = 1 \tag{10}$$

The PDF values were normalised such that the mean was zero and the variance was one for a relative comparison between the data values. The normalised PDF $\tilde{d}$, can be calculated as follows:

$$\tilde{d} = \frac{d_i - E_d}{\sigma_d} \tag{11}$$

where, d_i = 1, …, N represents the groundwater level data. The mean E_d and standard deviation σ_d are as follows:

$$E_d = \frac{1}{N}\sum_{i=1}^{N} d_i \tag{12}$$

$$\sigma_d = \sqrt{\left(\frac{1}{N}\sum_{i=1}^{N}(d_i - E_d)^2\right)} \tag{13}$$

The normalised PDF is converted into a cumulative density function (CDF) $F_x(x)$:

$$F_X(x) = P_X(X \leq x) \tag{14}$$

The quantile of the groundwater levels for a certain day corresponds to the percentage of the total data. The k-th q-quantile corresponds to the k-th data when the distribution of the data is evenly divided by q. Alternatively, when the data are sorted in ascending order, the k-th q-quantile corresponds to the groundwater data that correspond to k/q (%). This normalisation process projects a CDF value onto a standard normal-distribution CDF [31]. Finally, the SGLI value of the groundwater level on the horizontal axis was determined on the vertical axis by projecting the cumulative kernel density estimation (CKDE) into a standard normal quantile function.

The research design is plotted in Figure 1, illustrating from the start of grouping of groundwater level fluctuation based on the groundwater level characteristics and the river stage to determining the SGLI values of the wells.

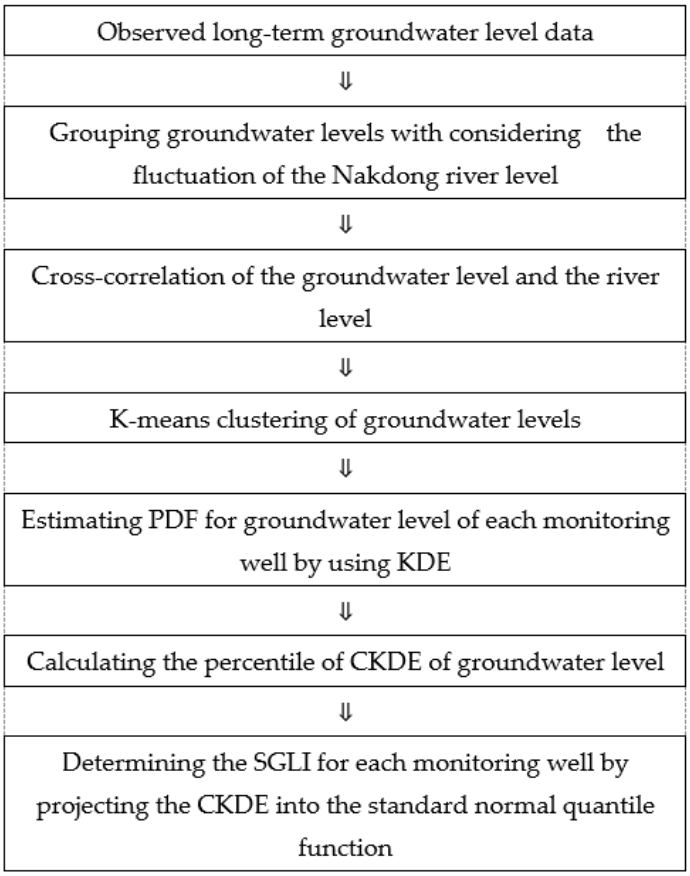

Figure 1. General research methodology flowchart of this study.

3. Study Area

3.1. Data Acquisition

The study area includes Changnyeong-gun County located at 128°21′–128°39′ longitude and 35°22′–35°40′ latitude and Haman-gun County located at 128°16′–128°35′ longitude and 35°09′–35°23′ latitude, just upstream of Changnyeong–Haman River barrage which is one of the eight barrages installed on Nakdong River (Figure 2). Changnyeong–Haman River barrage was completed on 10 December 2012, with an increase of groundwater level from an average of 1.36 m MSL in June 2011 to averages of 3.24 m MSL in December 2011 and 3.03 m MSL in January 2012, respectively, and the stabilization of groundwater level at ~4 m MSL (with averages of 4.45 m MSL in December 2012, 4.37 m MSL in January 2013, and 3.95 m MSL in December 2013) [17]. In fact, the Korean government launched the Four River Restoration Project in 2008 to construct 16 river barrages on four major rivers (the Han, Nakdong, Geum, and Yeongsan Rivers) that focused on proper management of flood control and effective water resource use to confront variable and heavy precipitation in summer, which partly results from climate change. During the Four River Restoration Project, at Changnyeong–Haman River barrage site, the original width of Nakdong River increased from 330 to 520 m and the elevation of the river bottom changed from –2.0 to –5.70 m MSL [32]. However, the Korean government initiated a new project for opening some of the 16 river barrages to restore the ecological environment of the rivers by reducing algae (chlorophyll-a) and improving the habitats of animals and plants. As a result, Changnyeong–Haman River barrage was opened during the following periods: 7–28 February 2017; 11–23 November 2017; 10 October–21 November 2018; 7 October–22 November 2019; and 10 October–22 November 2020.

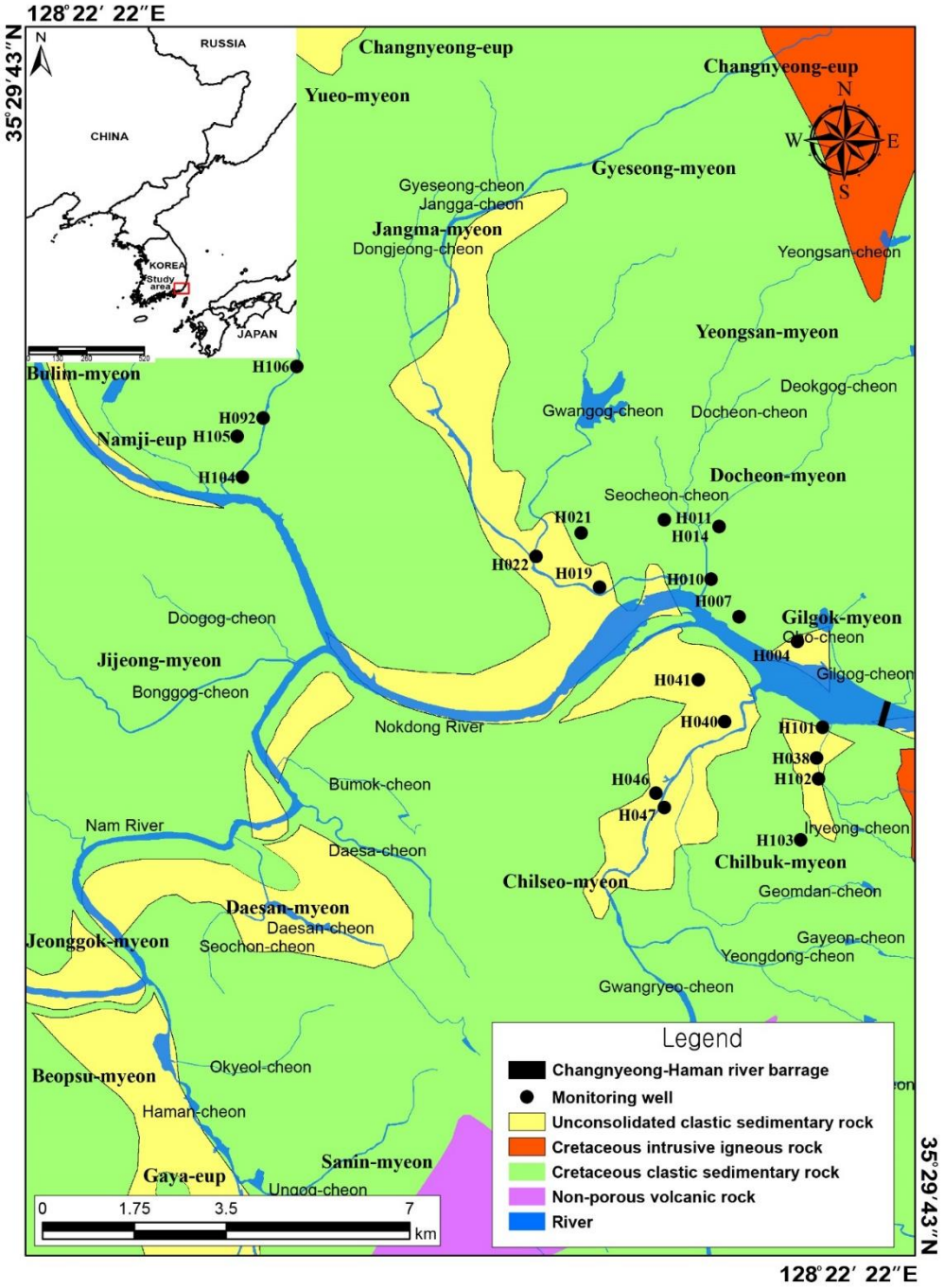

Figure 2. Location of the monitoring wells in the study area.

Around the right bank of Nakdong River and 2.8 km upstream of Changnyeong–Haman River barrage, in the Haman area, where the wells H040, H041, H046, and H047 are located, the topography is mostly flat with scattered small hills. Wells H014, H019, and H022 are located on the left bank of Nakdong River, 5 km upstream of the barrage. Wells H004 and H007 are located near the left bank of the river and directly upstream of the barrage in the Changnyeong area. The Chilseo rural industrial complex is located in the southwestern part of the country, and agricultural land is mainly located in the eastern part. Greenhouse cultivation has been the main agricultural activity since the completion of the barrage, whereas before the construction of the barrage, rice paddies were widely distributed in the study area. Various crops, such as red peppers, cucumbers, cherry tomatoes, and tomatoes, are cultivated in the greenhouse facilities. Red peppers,

cucumbers, pumpkins, rice, beans, garlic, green onions, and onions are grown in open fields. Groundwater is mainly used for water curtain cultivation in greenhouses and irrigation. Consequently, the groundwater level changed during the agricultural cycle of rice cultivation (May–August) and greenhouse agriculture (December–April) [20]. After the completion of the barrage, the amount of groundwater used drastically increased throughout the year. From November to March, groundwater is used intensively to raise the temperature inside greenhouses in the form of water curtains [33].

For analysing groundwater drought near the barrage, through the database of the K-water National Groundwater Information Centre, groundwater data were acquired from 20 wells (H004, H007, H010, H011, H014, H019, H021, H022, H038, H040, H041, H046, H047, H092, H101, H102, H103, H104, H105, and H106) that belong to the national groundwater monitoring network adjacent to Nakdong River. Both groundwater level and temperature were observed in the wells of the national groundwater monitoring network at hourly intervals. Most groundwater level data from the 20 wells were acquired from May 2012 to October 2020, including data from one well from January 2017 to October 2020 and five wells from June 2018 to October 2020.

3.2. Geological and Hydrological Settings

The geology of the study area (Figure 3) is composed of Cretaceous sedimentary rocks of the Hayang Group and Cretaceous volcanic rocks (mainly Jusan andesite) of the Yucheon Group belonging to the Gyeongsang Supergroup, with the intrusion of Cretaceous Bulguksa igneous rocks, including diorite, biotite granite, granodiorite, granite porphyry, and dikes [34–36]. Quaternary alluvial layers chiefly occurring along the river area are composed of clay, sand, gravel and weathered layers, in descending order, with an average thickness of 7.9 m, 9.1 m, 5.6 m and 5.1 m, respectively [20]. Cretaceous sedimentary rocks mainly consist of purple shale, grey shale, greenish-grey sandstone/sandy shale, and purple sandy shale. The Haman Formation, which belongs to the Hayang group, consists of purple shale, grey shale, greenish-grey sandstone, and sandy shale and is not frequently intercalated by andesite. Alluvial layers composed of clay, sand, and gravel are widely distributed around the Gwangryecheon and Gyeseongcheon streams and the tributary streams of Nakdong River.

Nakdong River runs from north to south and west to east. The Gwangnyeocheon stream flows from south to northeast into the river. The Gyeseongcheon stream flows into Nakdong River from Jangcheok Lake, Yudong Reservoir, and Bongsanji Reservoir. The Ohocheon stream flows from Naedong Reservoir to the river. Overall, the topography of this study area was formed by geological processes, such as structural activity, weathering, and erosion. The topography of the eastern part is composed of a floodplain consisting of rice paddies, the western part is composed of mountainous areas, such as Dochosan Mountain and Mabunsan Mountain, and the southern region adjacent to the river is an urban area. The topography is closely related to groundwater recharge and discharge. In this regard, groundwater storage and occurrence are governed by topography, geology, precipitation, and infiltration of surface water.

The floodplain, located in the eastern part of the basin, is used for rice paddy and greenhouse cultivation. To grow crops, the greenhouse was heated using a water curtain and boiler in winter. Cucumber, the main crop, is grown in greenhouses, whereas pepper, pumpkin, and rice are cultivated in open fields.

Precipitation recorded at Milryang Meteorological Observatory from 2012 to 2020 showed an average annual rate of 1179 mm, with the highest monthly mean of 216.4 mm in August and the lowest mean of 186.2 mm in September (Figure 4). The figure shows the highest monthly precipitation of 528.7 mm in August 2014 and the lowest monthly precipitation of 0 mm in November 2017.

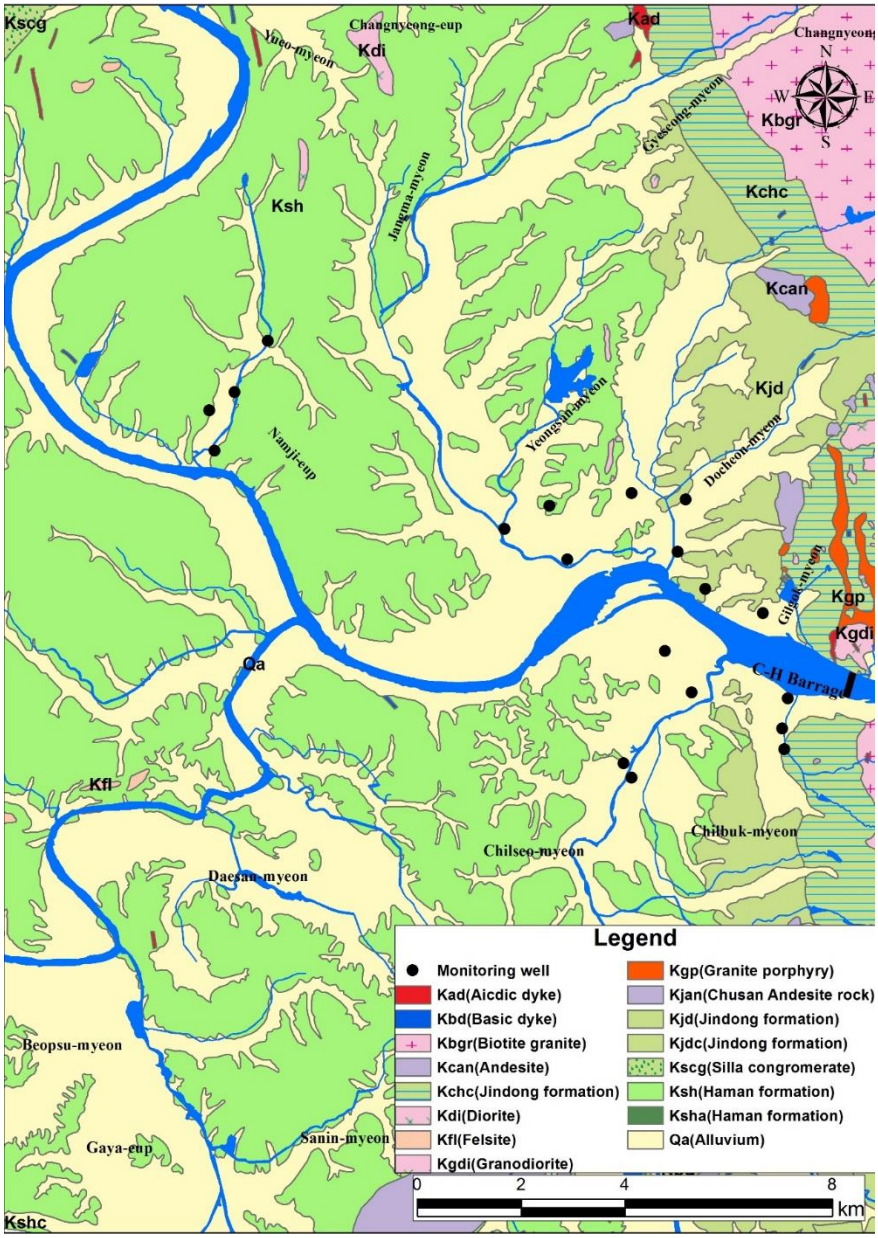

Figure 3. Geological map of the study area [34–36].

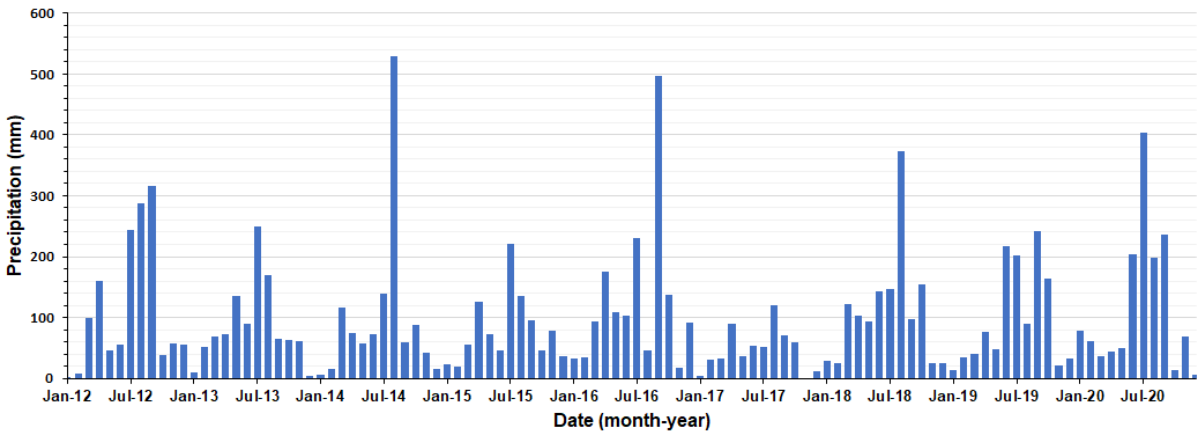

Figure 4. Monthly precipitation at Milryang Meteorological Observatory from 2012–2020.

4. Results

4.1. Characteristics of Groundwater Level and River Stage Fluctuation

As mentioned earlier, Changnyeong–Haman River barrage was opened during the following periods: 7–28 February 2017; 11 November to 23 December 2017; 10 October to 21 November 2018; 7 October to 22 November 2019; 10 October to 22 November 2020. By the opening of the barrage in the periods 11 November–23 December 2017 and 10 October–21 November 2018, the river stage exhibited drops of 1.5 m and 2.6 m, respectively (Figure 5). The figure shows the highest daily groundwater level of 11.38 m MSL in August 2020 and the lowest daily groundwater level of 2.06 m MSL in November 2018. The lowest river stage is 2.2 m MSL, and the management river stage is 5.0 m MSL, which is the maximum river level for controlling the barrage. Using groundwater levels from 20 wells, Groups 1, 2, and 3 were selected based on groundwater fluctuation patterns (Figure 6) and the cross-correlation between the groundwater level and river stage (Figure 7). In Figure 6, the groundwater levels range from 0.70–10.72 m MSL (an average of 4.57 m MSL) for Group 1, −1.63–12.20 m MSL (an average of 5.92 m MSL) for Group 2, and −10.20–24.35 m MSL (an average of 5.46 m MSL) for Group 3. In Figure 7, H004 displays lag times of 0 d with a prominent peak of 0.33, H007 displays lag times of 28 d with a prominent peak of 0.29, and H046 displays lag times of 171 d with a prominent peak of 0.45.

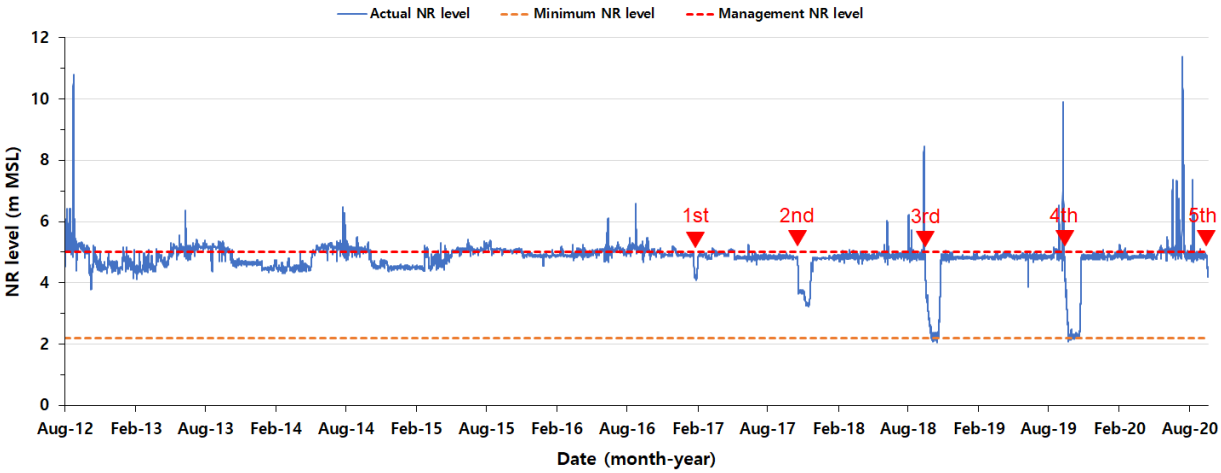

Figure 5. Stages of Nakdong River at Changnyeong–Haman River barrage from 2012 to 2020, with indication of the five barrage openings (red triangle).

Group 1 comprised wells H004, H019, H040, H041, H047, and H101, dominated by the fluctuation of the river level, and showed seasonal fluctuation of at most 2 m with a maximum 2-m decline in accordance with the drop in the river stage during the opening periods of the barrage, November 2017, October 2018, and October 2019. Well H019 displayed lower groundwater levels than river water levels, similar to the condition of a losing stream. Wells H004 and H101 are located at a distance of ~300 m from the river and wells H040 and H041 are at a distance of ~1 km from the river. Well H047 is located 85 m from the tributary and 2.9 km from the main river. According to the cross-correlation with every one-year offset for 2012–2020, the groundwater levels of wells H004, H019, H040, H041, H047, and H101 belonging to Group 1 displayed lag times of 0 d and indicated a sensitive response to the river stage change (Figure 7).

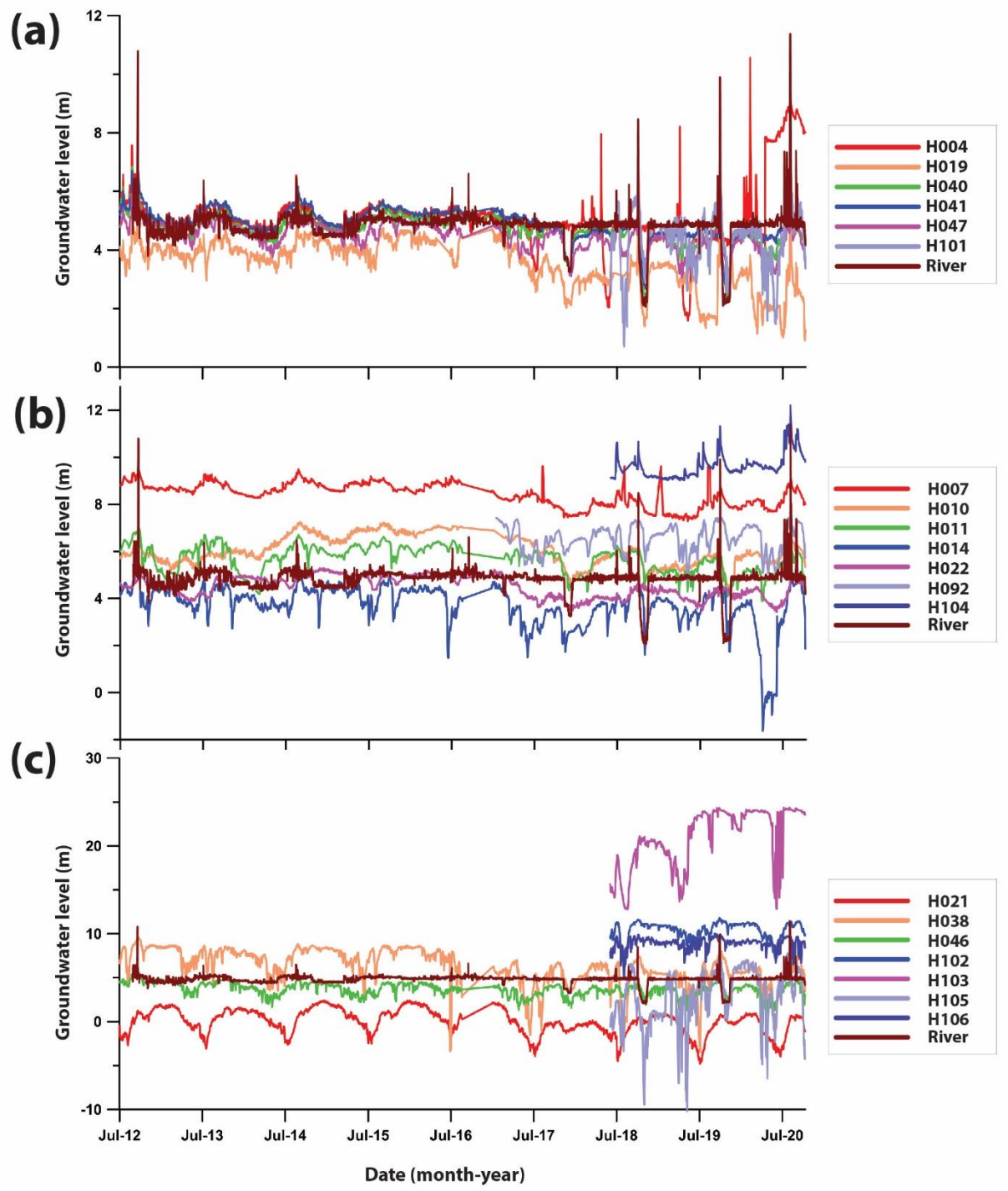

Figure 6. Representative groundwater-level fluctuations belonging to (**a**) Group 1, (**b**) Group 2, and (**c**) Group 3 in 2012–2020.

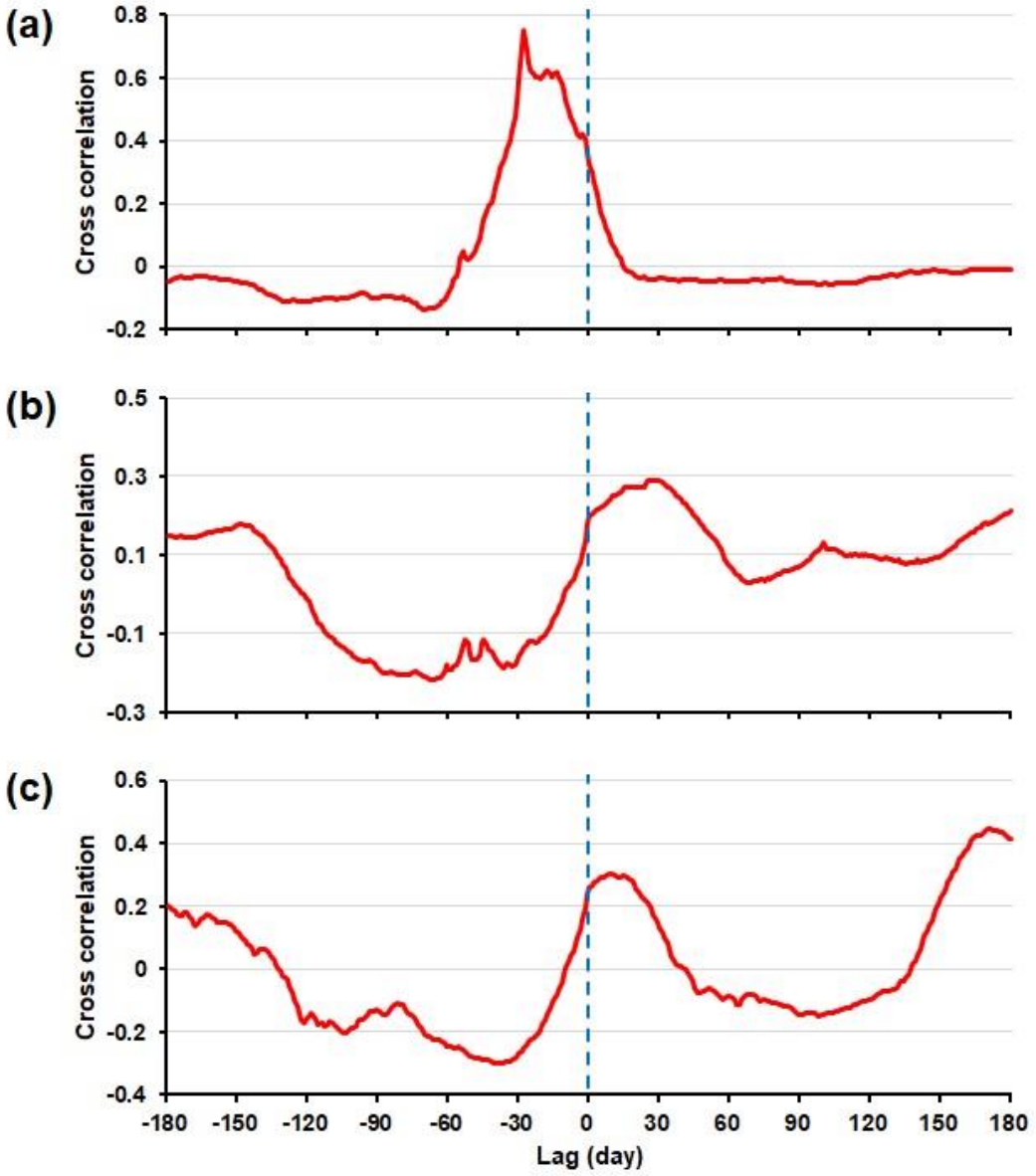

Figure 7. Cross correlation of the river level and groundwater level on (**a**) H004 (Group 1), (**b**) H007 (Group 2), and (**c**) H046 (Group 3).

Group 2,consisting of wells H007, H010, H011, H014, H022, H092, and H104 located within 300 m of the main river and tributary, was not directly affected by the main river water level and did not show an immediate reaction due to the opening of the barrage and showed no rapid increase in groundwater levels during the rainy season. However, because the distance of the wells from the river is relatively small, the annual groundwater-level change is maintained within approximately 3 m, with a continuous supply of water from the river. In particular, well H007 near the river did not exhibit a decline in groundwater level. This irrelevant response of the well may be due to the recharge into the alluvial aquifer from surface water storage near the drainage pumping station. The groundwater levels of wells H007, H010, H011, H014, H022, H092, and H104, which belong to Group 2, displayed lag times of 28 d, 14 d, 10 d, 172 d, 180 d, 177 d, and 26 d, respectively. This indicates that the influence of rivers on the wells appears to be less (Figure 7).

Group 3 comprised the other wells (H021, H038, H102, H103, H104, H105, and H106) and was less affected relatively by the opening of the barrage. Group 3 implies that wells 1 km from the river are less affected by the river, showing seasonal fluctuations greater than 3 m per year. In addition, there was no immediate drop in the groundwater level owing

to the opening of the barrage. The groundwater level of well H046 at a distance of ~3 km from the river and 130 m from the tributary was lower than that of the river stage and displayed a combined response due to rainfall and pumping from nearby wells, as well as the influence of the opening of the barrage (Figure 6). It was judged that well H021 with a deeper well depth demonstrated a smaller influence on the opening of the barrage owing to the influence of deeper aquifers. The groundwater levels of wells H021, H038, H046, H102, H103, H104, H105, and H106 belonging to Group 3 displayed lag times of 180 d, 180 d, 171 d, 180 d, 165 d, 2 d, and 177 d, respectively. The long lag time was due to the small response to river stage changes and large seasonal fluctuations in the groundwater level (Figure 7).

4.2. Clustering of Groundwater Levels

In the previous section, we grouped the groundwater levels into three groups based on the patterns of groundwater level fluctuations and cross-correlation. In this section, the daily groundwater data of the 20 monitoring wells for the period from June 2018 to October 2020 were grouped through K-means cluster analysis using the sum of the distances between the monitoring wells and were analysed to consider the effect of the opening of the barrage.

Using K-means cluster analysis, the groundwater level data were more precisely classified into five clusters (Table 1). Cluster 1 corresponds to Group 1. Clusters 2 and 3 roughly correspond to Group 2. Cluster 1 corresponds to H004, H010, H011, H022, H040, H041, H047, H092, and H101, with a range of 3.8–6.2 m in groundwater level. Cluster 2 implies H014, H019, H038, H046, and H105, with a range of −1.6–5.3 m in groundwater level. Cluster 3 involves H007, H102, H104, and H106 wells, with groundwater levels ranging from 8.0 to 10.2 m. Cluster 4 includes H021 with an average groundwater level of 9.8 m. Cluster 5 corresponds to H103, showing an average groundwater level of 23 m.

Table 1. Result of K-means cluster analysis results.

Cluster	Monitoring Wells
Cluster 1	H004, H010, H011, H022, H040, H041, H047, H092, H101
Cluster 2	H014, H019, H038, H046, H105
Cluster 3	H007, H102, H104, H106
Cluster 4	H021
Cluster 5	H103

4.3. KDE and CKDE of Groundwater Level

KDE and CKDE were computed for groundwater levels belonging to Clusters 1 to 5. KDE and CKDE versus groundwater level were examined for Clusters 1–3, exempting Clusters 4 and 5. In Figure 8, the horizontal axis represents the groundwater level, and the vertical axis represents KDE and CKDE. In this figure, H004 shows a prompter change in the slope of the CKDE than H014 and H021.Wells H004, H014, H040, H041, H047, and H106 belonging to Cluster 1 showed a rapid increase in CKDE with increasing groundwater levels due to a rapid response to the river level discerned by cluster analysis (Figure 8). In this figure, the KDE peak for the periods excluding the opening of the barrage was higher than that for the total period. Wells H014, H019, H038, H046, and H105 belonging to Cluster 2 demonstrated a slower increase in CKDE than those in Cluster 1 (Figure 8). Finally, wells H007, H102, H104, and H106, belonging to Cluster 3, displayed the slowest increase in CKDE, with a gentle peak. An abrupt change in the slope of the cumulative probability density, such as that in Cluster 1, occurs when the groundwater level is relatively high, low, or distributed around the median value owing to external factors (pumping, barrage opening, or rainfall). In particular, the relatively low groundwater levels of wells H004, H040, and H041 belonging to Cluster 1 are considered to be caused by the relatively wide range of groundwater level decline due to the opening of the barrage.

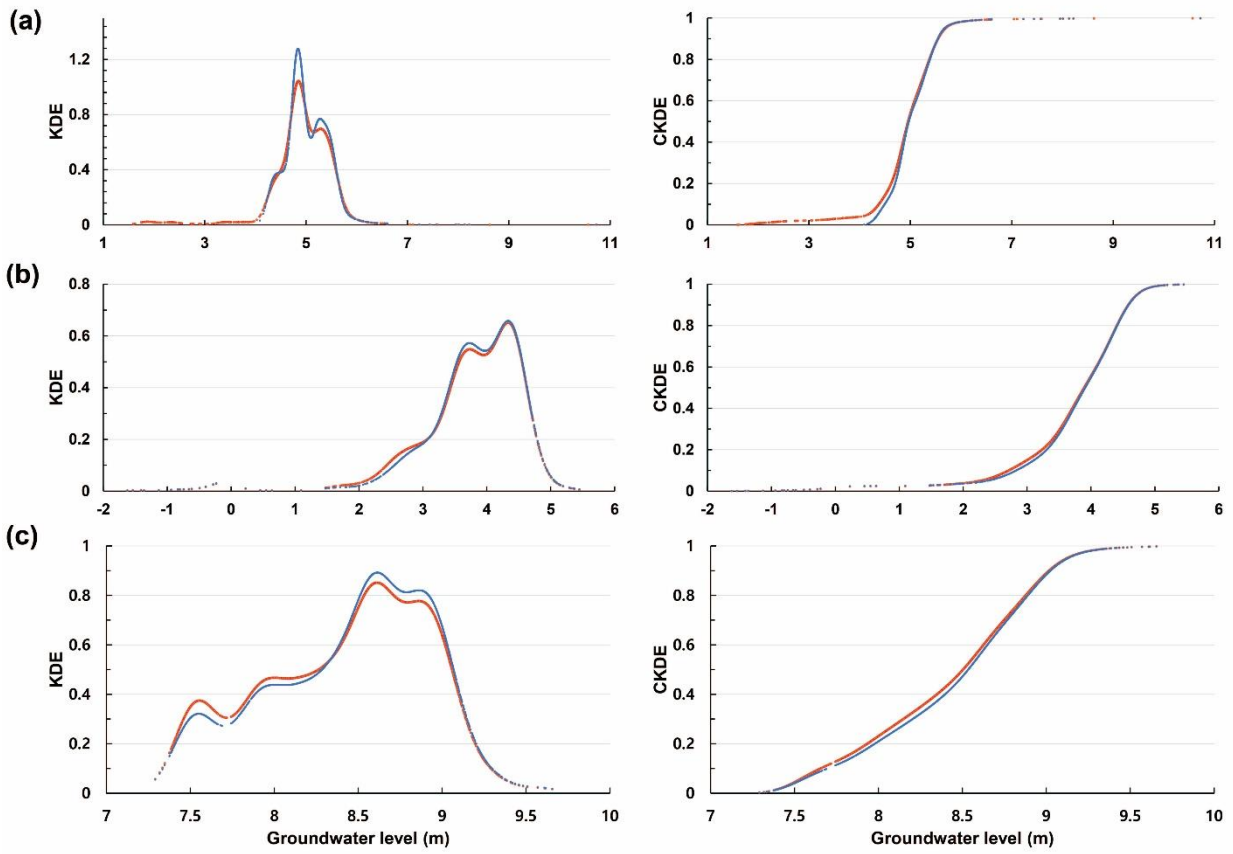

Figure 8. KDE and CKDE versus groundwater level of the wells (**a**) H004, (**b**) H014, and (**c**) H021 for the total period of July 2012−October 2020 (red colour) and those for the periods excluding the opening of the barrage (blue colour).

The annual KDE values for wells H004, H014, and H007 from July 2012 to June 2020 show that the effect of barrage construction appears from 2015 (Figure 9). At the well H004 belonging to Cluster 1, according to seasonal influence, the groundwater level fluctuated from 4.5 m to 6.5 m MSL with a range of 2 m during the period of July 2012–June 2015, the period before the installation of the barrage. In contrast, from July 2015 (after the installation of the barrage) to June 2020, the groundwater level fluctuation decreased by approximately 1 m. Additionally, the groundwater level was in the range of 5–6 m MSL in 2015 and gradually decreased to 4–5 m MSL in 2019. The KDE of H004 increases with decreasing groundwater level year by year. In contrast, the KDE of H014 decreases with decreasing groundwater level year by year. The KDE of H007 shows a decreasing tendency with slightly decreasing groundwater level year by year.

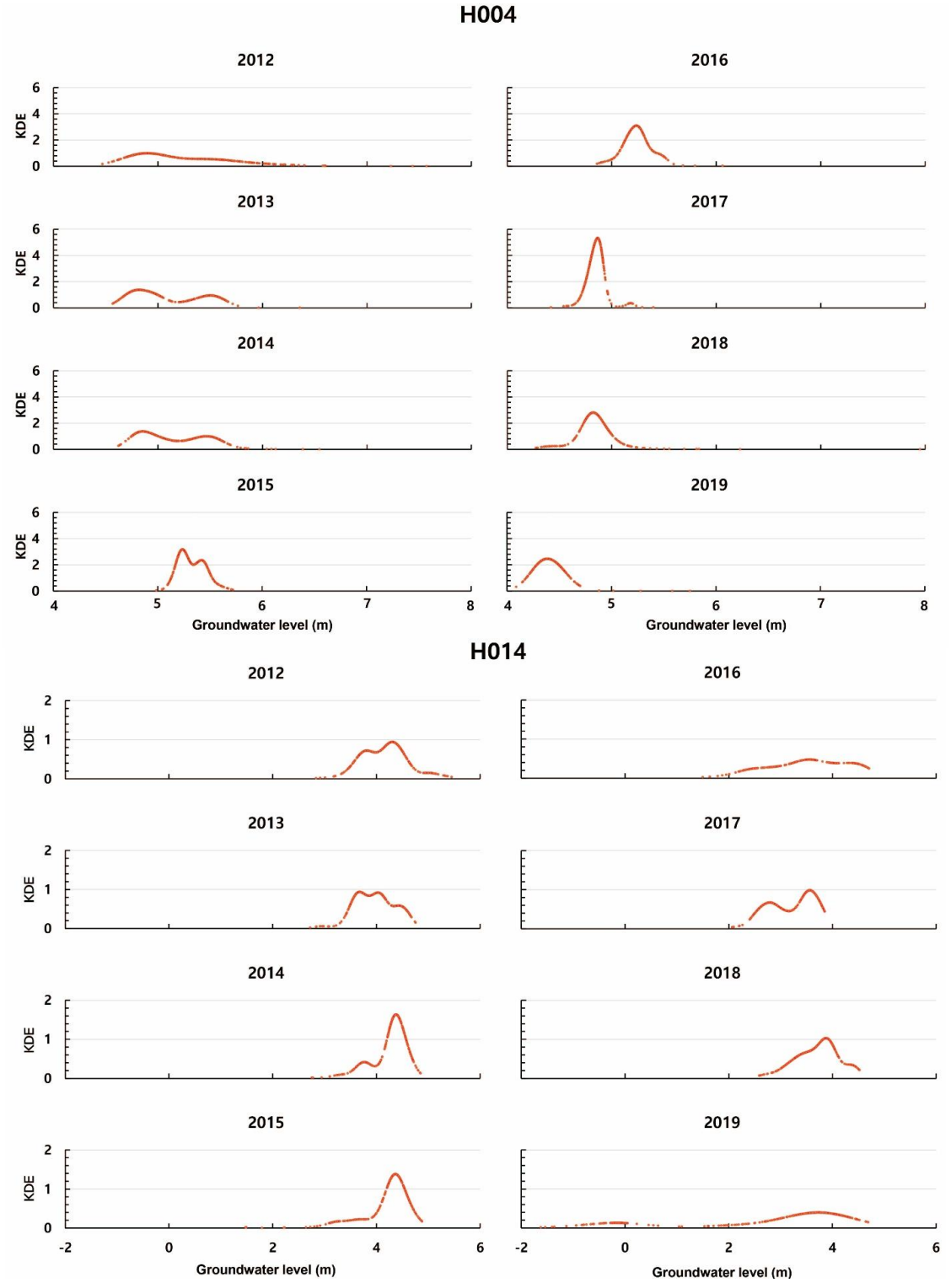

Figure 9. *Cont.*

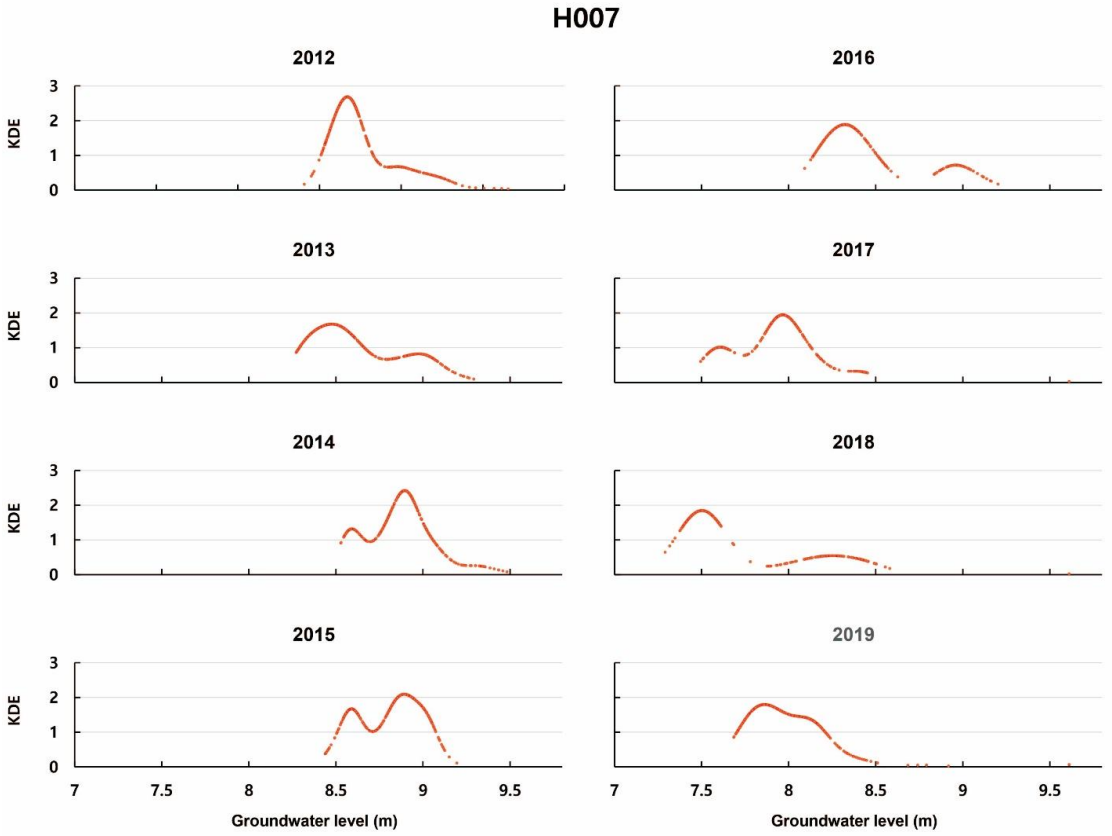

Figure 9. KDE versus groundwater level of H004 (Cluster 1), H014 (Cluster 2), and H007 (Cluster 3) on an annual basis from July 2012 to June 2020.

For well H014 belonging to Cluster 2, due to seasonal influence, the groundwater level ranged from 2.5 to 5.5 m MSL during the period of July 2012–June 2016, the period before the installation of the barrage. In contrast, from July 2015 (since the construction of the barrage) to June 2020, the groundwater level was between 2 and 4 m MSL. Additionally, the groundwater level was in the range of 2–5 m MSL in 2015, 2–4.5 m MSL from 2016 to 2018, and −1–5 m MSL in 2019, with a decreasing tendency.

For well H007 belonging to Cluster 3, from July 2012 to June 2016 before the opening of the barrage, the groundwater level was 8.3 to 9.6 m MSL, with an annual fluctuation of ~1.0 m MSL due to seasonal effect. In contrast, from July 2016 to June 2019 after the opening of the barrage, the annual groundwater level change was about 7.3 to 8.8 m MSL.

4.4. Estimation of the SGLI Values

SGLI Values Depending on the Opening of the Changnyeong–Haman River Barrage

The SGLI values from the CKDE values were computed for the period from July 2012 to October 2020, including the five opening periods (Figure 10). Groundwater drought stages were classified using a statistical technique of percentiles or normalised indices. The stage of caution was set at 25th or lower when using percentiles. When normalised indices are used, drought stages are classified into −1, −1.5, −2, and so on. In this study, the boundaries of groundwater drought for the caution, severe, and very severe stages, and SGLI values of −0.674, −1.282, and −1.645 corresponding to the 25th, 10th and 5th percentiles, respectively, are adopted as the drought forecasting and warning system. In Figure 10, for the period before the opening of the barrage, the SGLI values ranged −1.34 to 3.54 (a mean of 0.46) for H004, ranged −1.92 to 3.10 (a mean of 0.41) for H014, and ranged −0.46 to 2.95 (a mean of 0.59) for H007. In contrast, for the periods of the barrage opening, the SGLI values ranged −2.93 to 3.27 (a mean of −0.60) for H004, ranged −3.37 to 1.93 (a mean of −0.56) for H014, and ranged −2.73 to 2.81 (a mean of −0.83) for H007.

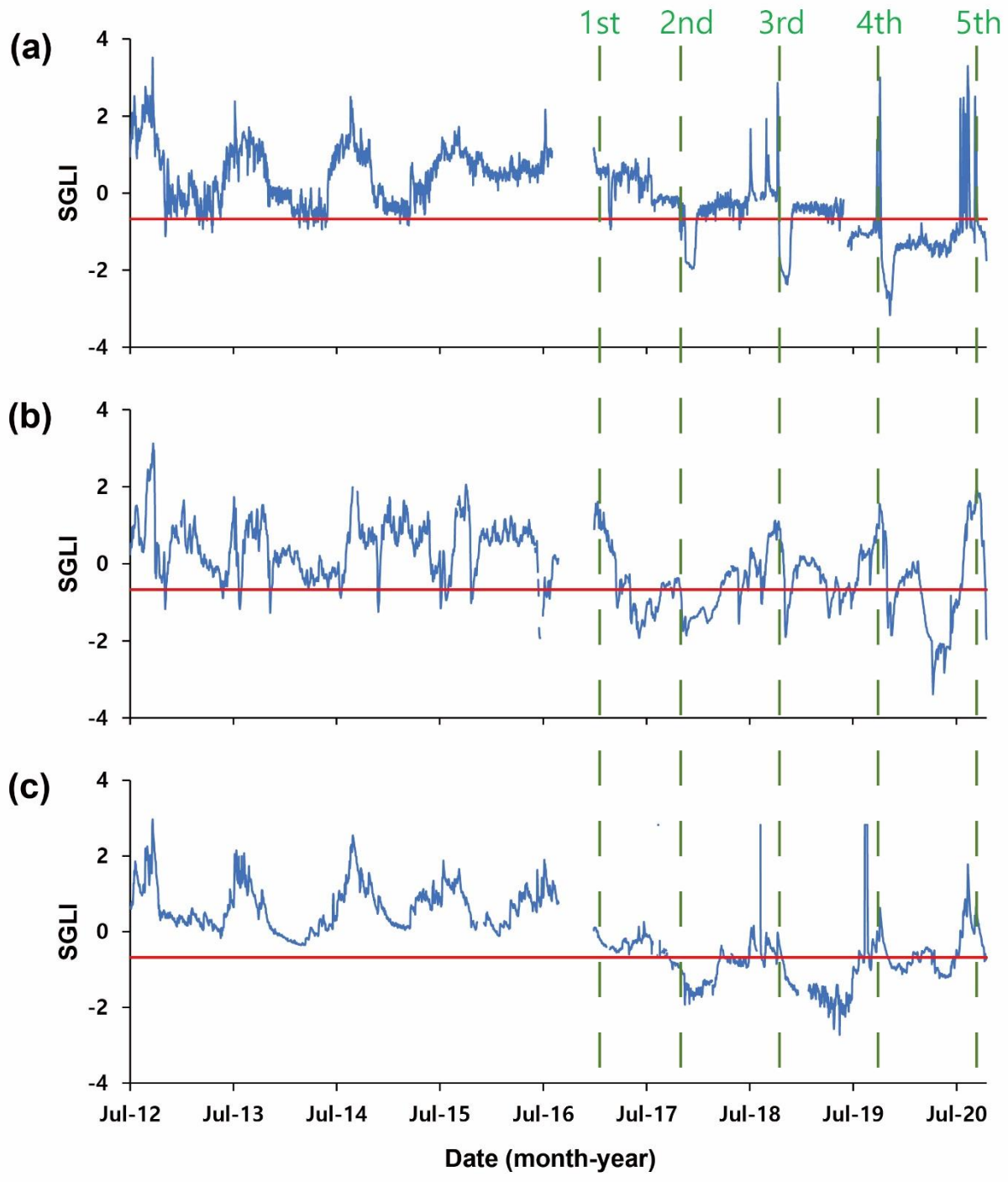

Figure 10. SGLI values of (**a**) H004, (**b**) H014, and (**c**) H007, respectively belonging to Cluster 1, 2, and 3, for the periods of 2012−2020. Red line indicates 25th percentile (−0.674) of SGLI values. The vertical dash line in green colour indicates the time of the barrage opening.

The SGLI values for the period before the opening of the barrage (July 2012 to February 2017) ranged from −3.15 to 3.56 whereas the SGLI values during opening period (February 2017 to October 2020) ranged from −3.55 to 3.35 (Tables 2 and 3). This indicates a higher groundwater drought potential in the opening period of the barrage than the period before the opening of the barrage.

Table 2. Statistic of SGLI for the period before the opening of the barrage (July 2012 to February 2017).

Static.	**H004**	**H007**	**H010**	**H011**	**H014**	**H019**	**H021**	**H022**	**H038**	**H040**
Min.	−1.34	−0.46	−1.59	−2.52	−1.92	−0.90	−1.82	−1.17	−3.15	−1.48
Max.	3.54	2.95	2.42	3.10	3.10	3.55	2.18	2.42	2.79	3.54
Mean	0.46	0.59	0.42	0.39	0.41	0.58	0.40	0.56	0.51	0.47
Static.	H041	H046	H047	H092	H101	H102	H103	H104	H105	H106
Min.	−0.85	−2.33	−1.54	1.29	-	-	-	-	-	-
Max.	3.40	3.56	3.56	1.90	-	-	-	-	-	-
Mean	0.54	0.32	0.49	1.62	-	-	-	-	-	-

Table 3. Statistic of SGLI for the periods of the barrage opening (February 2017 to October 2020).

Static.	**H004**	**H007**	**H010**	**H011**	**H014**	**H019**	**H021**	**H022**	**H038**	**H040**
Min.	−2.93	−2.73	−3.05	−3.23	−3.37	−3.02	−3.19	−3.06	−3.26	−3.55
Max.	3.27	2.81	0.74	1.46	1.93	3.12	1.42	1.63	0.70	3.27
Mean	−0.60	−0.83	−0.59	−0.51	−0.56	−0.81	−0.55	−0.74	−0.73	−0.64
Static.	H041	H046	H047	H092	H101	H102	H103	H104	H105	H106
Min.	−3.19	−3.37	−3.41	−3.04	−3.02	−2.97	−2.15	−1.48	−3.03	−3.17
Max.	3.35	2.46	3.11	2.81	3.18	2.48	1.10	3.18	2.40	2.53
Mean	−0.72	−0.42	−0.67	−0.04	−0.01	−0.03	−0.04	0.03	−0.02	−0.02

During the opening of the barrage, the SGLI values of wells H004, H040, and H041 lie in the domain where the groundwater level is relatively low, indicating a greater effect on the groundwater level of the three wells due to the lowering of Nakdong River stage by the barrage (Figure 10). In the circumstance that Cluster 1 and Cluster 2 respond to the variation in Nakdong River stages as tributaries fall below the 25th percentile in the period as well as the five opening periods of the barrage, the SGLI values of wells H004 (Cluster 1) and H014 (Cluster 2) fall below the 25th percentile in addition to the five opening periods of the barrage. In contrast, since Cluster 3 is not directly affected by Nakdong River stages and does not show an immediate response with the opening of the barrage, the SGLI values of well H007 belonging to Cluster 3 were mostly above the 25th percentile, except during the five opening periods of the barrage. Therefore, more care should be taken to maintain the groundwater level above the 25th percentile of SGLI values during the opening of the barrage.

5. Discussion

In the study area, groundwater levels of the monitoring wells, from June 2011 to January 2014 before the construction of the barrage, were classified into Group 1 (that is mainly influenced by the river level fluctuation) and Group 2 (that is mostly influenced by pumping) [19]. In contrast, from May 2012 to October 2020, Group 1 exhibited a maximum seasonal fluctuation of 2 m, with variations in Nakdong River stages. Group 2, which was located within 300 m of the main Nakdong River and tributary, was not directly affected by the main Nakdong River stage and did not show an immediate reaction to the opening of the barrage, with no rapid increase in the groundwater level during the rainy season. Group 3, covering wells 1 km from Nakdong River, was less affected relatively by the opening of the barrage and is less affected by Nakdong River, showing a seasonal fluctuation greater than 3 m annually.

British Columbia defines four drought response levels using four core indicators (basin snow indices, seasonal volume runoff forecasts, 30-day-percent average precipitation, and 7-day average streamflow): Level 1 (green) under normal conditions, Level 2 (yellow) under dry conditions, Level 3 (orange) under very dry conditions, and Level 4 (red) under extremely dry conditions [37]. The thresholds of the core indicators were as follows: <45%

of normal for seasonal volume runoff forecasts, <25% of normal for 30-day percent average precipitation, and <6 percentiles for 7-day average streamflow.

Non-parametric normalisation of data assigns a value to groundwater levels based on their rank within a dataset, in which case, groundwater levels for a given month from a given hydrograph (note that this normalisation routine is equally applicable to timescales larger than one month). The normal scores transform is undertaken by applying the inverse normal cumulative distribution function to n with equally spaced pi values ranging from $1/(2n)$ to $1 - 1/(2n)$. The resulting values are the SGLI values. Lee et al. [38] calculated the SGLI values for the normal, caution, severe, and very severe stages of groundwater drought in Korea using monthly groundwater level data. In this study, we identified the groundwater level characteristics and groundwater drought that depend on the opening of the barrage. In addition, because South Korea does not have recognisable snow, we considered only streamflow and groundwater levels to indicate groundwater drought. The SGLI values during opening period ranged from 3.35 to −3.55. In contrast, groundwater drought in the dry season in 1995 in U.S. was severe with a minimum SGI value of −2.539 with excessive pumping for agricultural activity [39]. This means that severe groundwater drought in the study area can take place with the opening of the barrage.

The uncertainty of SGLI value can be substantial. Therefore, in order to improve the accuracy of the SGLI, it is necessary to use other approaches such as nonparametric methods, ensemble approaches, or probability-based indices based on extreme-value statistics [40].

6. Conclusions

In this study, we characterised the groundwater level and Nakdong River stages from May 2012 to October 2020 and evaluated groundwater drought with the opening of Changnyeong–Haman River barrage. The characteristics of groundwater-level fluctuations due to the construction of the barrage near Nakdong River were unveiled. Groundwater level fluctuations were characterised by two steps: observational grouping and K-means clustering. First, the observational grouping of the groundwater level changes in relation to the fluctuation in Nakdong River stages resulted in three groups (Groups 1, 2, and 3). Group 1, comprising wells H004, H019, H040, H041, H047, and H101, exhibited seasonal fluctuations of at most 2 m with a maximum 2-m decline in accordance with the variation of Nakdong River stages. The cross-correlation of the groundwater level and Nakdong River stage also showed a stronger relationship with a short lag time. Group 2 implies that the H007, H010, H011, H014, H022, H092, and H104 wells, which are located within 300 m of the main Nakdong River and tributary, were not directly affected by the main Nakdong River level and did not show an immediate reaction to the opening of the barrage, with no rapid rise in groundwater level during the rainy season. Group 3, covering wells 1 km from Nakdong River, H021, H038, H102, H103, H104, H105, and H106, was less affected relatively by the opening of the barrage and is less affected by the river, showing a seasonal fluctuation greater than 3 m annually.

Secondly, the K-means cluster analysis verified five clusters (Clusters 1, 2, 3, 4, and 5) that represent the groundwater levels more precisely than using groundwater fluctuation patterns and the cross-correlation of the groundwater level versus Nakdong River stage. Cluster 1 corresponds approximately to Group 1, and Clusters 2 and 3 correspond approximately to Group 2. This means that Group 2 can be further divided into Clusters 2 and 3. In Cluster 1, the groundwater level increased rapidly with increasing CKDE. In addition, the KDE peak for the periods excluding the opening of the barrage was higher than that for the entire period including the opening of the barrage. In contrast, Cluster 2 demonstrated a slower increase in CKDE than Cluster 1 did. Cluster 3 displayed the slowest increase in CKDE, with the gentlest peak.

In this study area, the SGLI criteria of groundwater drought were −0.674 (caution), −1.282 (severe), and −1.645 (very severe), respectively, corresponding to the 25th, 10th, and 5th percentiles. The SGLI values of Cluster 1 and Cluster 2, which respond with the variation of Nakdong River stages and tributaries, fall below the 25th percentile in the

period as well as the five opening periods of the barrage. In contrast, the SGLI values of Cluster 3, which is not directly affected by Nakdong River stages and does not show an immediate response with the opening of the barrage, are mostly above the 25th percentile in the period except the five opening periods of the barrage. According to the SGLI values, the monitoring wells mostly lie above the 25th percentile, while during the five opening periods of the barrage, the monitoring wells falls below the 25th percentile. Correspondingly, groundwater level above the 25th percentile of SGLI values should be maintained carefully during the periods of the opening of the barrage. Therefore, the SGLI values can effectively be adopted to a similar case of river barrage operation for groundwater drought forecasting and warning system.

Though the SGLI can effectively assess groundwater drought, in order to reduce the uncertainty of SGLI values, we need to use nonparametric methods, ensemble approaches, or probability-based indices based on extreme-value statistics.

Author Contributions: Conceptualisation, S.-M.Y., J.-H.J. and S.-Y.H.; methodology, J.-H.J., S.-M.Y., J.-Y.C. and S.-Y.H.; software, S.-M.Y., J.-H.J. and J.-Y.C.; validation, J.-Y.C. and S.-Y.H.; writing, original draft preparation, S.-M.Y., J.-H.J. and J.-Y.C.; writing, review, and editing, J.-Y.C. and S.-Y.H.; visualisation, S.-M.Y. and H.-T.J. Supervision, S.-Y.H. Project administration, S.-Y.H. Funding acquisition, S.-Y.H. All authors have read and agreed to the published version of the manuscript.

Funding: This study was financially supported by the National Research Foundation of Korea (NRF) grant funded by the Ministry of Science and ICT (2020R1A2B5B02002198).

Data Availability Statement: We used the data from Korea Water Resources Corporation that has the authority of the data.

Conflicts of Interest: The authors declare no conflict of interest.

References

1. World Meteorological Organization (WMO). *Manual on Estimation of Probable Maximum Precipitation (PMP)*; WMO-No. 1045; World Meteorological Organization (WMO): Geneva, Switzerland, 2009; 259p.
2. McKee, T.B.; Doesken, N.J.; Kleist, J. The Relationship of Drought Frequency and Duration to Time Scales. In Proceedings of the 8th Conference on Applied Climatology, Anaheim, CA, USA, 17–22 January 1993; pp. 179–183.
3. Van Lanen, H.A.; Peters, E. Definition, Effects and Assessment of Groundwater Droughts. In *Drought and Drought Mitigation in Europe*; Springer: Berlin/Heidelberg, Germany, 2000; pp. 49–61.
4. Peters, E.; Van Lanen, H.A.J.; Torfs, P.J.J.F.; Bier, G. Drought in groundwater-drought distribution and performance indicators. *J. Hydrol.* **2005**, *306*, 302–317. [CrossRef]
5. Mishra, A.K.; Singh, V.P. Drought modeling—A review. *J. Hydrol.* **2011**, *403*, 157–175. [CrossRef]
6. Bloomfield, J.P.; Marchant, B.P. Analysis of groundwater drought building on the standardised precipitation index approach. *Hydrol. Earth Syst. Sci.* **2013**, *17*, 4769–4787. [CrossRef]
7. Rahim, A.; Khan, K.; Akif, A.; Jamal, R. The geostatistical approach to assess the groundwater drought by using standardized water level index (SWI) and standardized precipitation index (SPI) in the Peshawar regime of Pakistan. *Sci. Int.* **2015**, *27*, 4111–4117.
8. Mendicino, G.; Senatore, A.; Versace, P. A groundwater resource index (GRI) for drought monitoring and forecasting in a Mediterranean climate. *J. Hydrol.* **2008**, *357*, 282–302. [CrossRef]
9. Kumar, R.; Musuuza, J.L.; Van Loon, A.F.; Teuling, A.J.; Barthel, R.; Ten Broek, J.; Mai, J.; Samaniego, L.; Attinger, S. Multiscale Evaluation of the standardized precipitation index as a groundwater drought indicator. *Hydrol. Earth Syst. Sci.* **2016**, *20*, 1117–1131. [CrossRef]
10. Bidwell, V.J. Realistic forecasting of groundwater level, based on the eigenstructure of aquifer dynamics. *Math. Comput. Simulat.* **2005**, *69*, 12–20. [CrossRef]
11. Goodarzi, M.; Fatehifar, A.; Avazpoor, F. Bivariate analysis of the impact of climate change on drought with SPEI index and Coppola functions (Case study: Dugonbadan). *Iran-Water Resour. Res.* **2019**, *15*, 352–365.
12. Osman, A.I.A.; Ahmed, A.N.; Chow, M.F.; Huang, Y.F.; El-Shafie, A. extreme gradient boosting (Xgboost) model to predict the groundwater levels in Selangor Malaysia. *Ain Shams Eng. J.* **2021**, *12*, 1545–1556. [CrossRef]
13. Osman, A.I.A.; Ahmed, A.N.; Huang, Y.F.; Kumar, P.; Birima, A.H.; Sherif, M.; Sefelnasr, A.; Ebraheemand, A.A.; El-Shafie, A. Past, present and perspective methodology for groundwater modeling-based machine learning approaches. *Arch. Compu. Methods Eng.* **2022**, *29*, 3843–3859. [CrossRef]
14. Song, S.H.; Lee, H.S.; Choi, K.J.; Kim, J.S.; Kim, G.P. Evaluation of drought effect on groundwater system using groundwater level data in Jeju Island. *J. Environ. Sci. Int.* **2014**, *23*, 637–647. [CrossRef]

15. Yang, J.S.; Par, J.H.; Kim, N.K. Development of drought vulnerability index using trend analysis. *Korean Soc. Civ. Eng.* **2014**, *32*, 185–192.
16. Kim, G.-B.; Yun, H.-H.; Kim, D.-H. Relationship between standardized precipitation index and groundwater levels: A proposal for establishment of drought index wells. *J. Soil Groundwater Environ.* **2006**, *11*, 31–42.
17. Huntington, J.L.; Niswonger, R.G. Role of surface-water and groundwater interactions on projected summertime streamflow in snow dominated regions: An integrated modeling approach. *Water Resour. Res.* **2012**, *48*, W11524. [CrossRef]
18. Menció, A.; Galán, M.; Boix, D.; Mas-Pla, J. Analysis of stream-aquifer relationships: A comparison between mass balance and Darcy's law approaches. *J. Hydrol.* **2014**, *517*, 157–172. [CrossRef]
19. Oh, Y.-Y.; Hamm, S.-Y.; Kim, G.B.; Lee, C.-M.; Chung, S.Y. Statistical approach to river–aquifer interaction in the Lower Nakdong River Basin, Republic of Korea. *Irrig. Drain.* **2016**, *65*, 36–47. [CrossRef]
20. Oh, Y.-Y.; Hamm, S.-Y.; Ha, K.; Yoon, H.; Chung, I.M. Characterising the impact of river barrage construction on stream–aquifer interactions, Korea. *Water.* **2016**, *8*, 137. [CrossRef]
21. Oh, Y.-Y.; Hamm, S.-Y.; Ha, K.; Yoon, H.; Kim, G.-B. Analytical approach for evaluating the effects of river barrages on river aquifer interactions. *Hydrol. Process.* **2016**, *30*, 3932–3948. [CrossRef]
22. Oh, Y.-Y.; Yun, S.-T.; Yu, S.; Hamm, S.-Y. The combined use of dynamic factor analysis and wavelet analysis to evaluate latent factors controlling complex groundwater level fluctuations in a riverside alluvial aquifer. *J. Hydrol.* **2017**, *555*, 938–955. [CrossRef]
23. Rosenberry, D.O.; LaBaugh, J.W. *Field Techniques for Estimating Water Fluxes between Surface Water and Ground Water: U.S. Geological Survey Techniques and Methods*; USGS: Reston, VA, USA, 2008; 128p.
24. Sophocleous, M. Interactions between groundwater and surface water: The state of the science. *Hydrogeol. J.* **2002**, *10*, 52–67. [CrossRef]
25. Zhu, M.; Wang, S.; Kong, X.; Zheng, W.; Feng, W.; Zhang, X.; Yuan, R.; Song, X.; Sprenger, M. Interaction of surface water and groundwater influenced by groundwater over-extraction, wastewater discharge, and water transfer in Xiong'an New Area, China. *Water* **2019**, *11*, 539. [CrossRef]
26. Jenkins, G.M.; Watt, D.G. *Spectral Analysis and Its Application*; Holden-Day Inc.: San Francisco, CA, USA, 1968; 525p.
27. Box, G.E.P.; Jenkins, G.M.; Reinsel, G.C. *Time Series Analysis: Forecasting and Control*, 3rd ed.; Prentice-Hall: Englewood Cliffs, NJ, USA, 1994; 598p.
28. Larocque, M.; Mangin, A.; Razack, M.; Banton, O. Contribution of correlation and spectral analyses to the regional study of a large karst aquifer (Charente, France). *J. Hydrol.* **1998**, *205*, 217–231. [CrossRef]
29. Sakoe, H.; Chiba, S. Dynamic programming algorithm optimization for spoken word recognition. *IEEE Trans. Acoust. Speech Signal Process* **1978**, *26*, 43–49. [CrossRef]
30. Silverman, B.W. *Density Estimation for Statistics and Data Analysis*; CRC Press: Boca Raton, FL, USA, 1986; p. 26.
31. Bolstad, B.M.; Irizarry, R.A.; Åstrand, M.; Speed, T.P.A. Comparison of normalization methods for high density oligonucleotide array data based on variance and bias. *Bioinformatics* **2003**, *19*, 185–193. [CrossRef] [PubMed]
32. Ministry of Land, Transportation, and Maritime Affairs (MLTM). *The Detail Design of Development of Residential Sites for Nakdong River District*; MLTM: Seoul, Republic of Korea, 2009.
33. Chang, S.; Chung, I.-M.; Kim, Y.; Moon, S.-H. Long-term groundwater budget analysis based on integrated hydrological model for water curtain cultivation site: Case study of Cheongweon, Korea. *J. Geol. Soc. Korea* **2016**, *52*, 201–210. [CrossRef]
34. Kim, N.J.; Lee, H.K. *Explanatory Text of the Geological Map of Yongsan Sheet (1:50,000)*; Geological Survey Korea: Seoul, Republic of Korea, 1964; 52p.
35. Choi, S.O.; Yeo, S.C. *Explanatory Text of the Geological Map of Namji Sheet (1:50,000), Sheet-6820-II*; Geological Survey Korea: Seoul, Republic of Korea, 1972; 27p.
36. Choi, Y.K.; Kim, T.Y. *Explanatory Text of the Geological Map of Uiryong Sheet (1:50,000)*; Geological Survey Korea: Seoul, Republic of Korea, 1963; 29p.
37. Economics. *British Columbia Drought Response Plan*; British Columbia: Victoria, BC, Canada, 2015; p. 35.
38. Lee, J.; Kang, S.; Jeong, J.; Chun, G. Development of groundwater level monitoring and forecasting technique for drought analysis (I)—Groundwater drought monitoring using standardized groundwater level index (SGI). *J. Korea Water Resour. Assoc.* **2018**, *51*, 1011–1020.
39. Guo, M.; Weifeng Yue, W.; Wang, T.; Zheng, N.; Wu, L. Assessing the use of standardized groundwater index for quantifying groundwater drought over the conterminous US. *J. Hydrol.* **2021**, *598*, 126227. [CrossRef]
40. Laimighofer, J.; Laaha, G. How standard are standardized drought indices? Uncertainty components for the SPI & SPEI case. *J. Hydrol.* **2022**, *613*, 128385.

Disclaimer/Publisher's Note: The statements, opinions and data contained in all publications are solely those of the individual author(s) and contributor(s) and not of MDPI and/or the editor(s). MDPI and/or the editor(s) disclaim responsibility for any injury to people or property resulting from any ideas, methods, instructions or products referred to in the content.